Since January 2020 Elsevier has created a COVID-19 resource centre with free information in English and Mandarin on the novel coronavirus COVID-19. The COVID-19 resource centre is hosted on Elsevier Connect, the company's public news and information website.

Elsevier hereby grants permission to make all its COVID-19-related research that is available on the COVID-19 resource centre - including this research content - immediately available in PubMed Central and other publicly funded repositories, such as the WHO COVID database with rights for unrestricted research re-use and analyses in any form or by any means with acknowledgement of the original source. These permissions are granted for free by Elsevier for as long as the COVID-19 resource centre remains active.

Journal of the Indian Chemical Society 99 (2022) 100433

Contents lists available at ScienceDirect

Journal of the Indian Chemical Society

journal homepage: www.journals.elsevier.com/journal-of-the-indian-chemical-society

An *In Silico* investigation for acyclovir and its derivatives to fight the COVID-19: Molecular docking, DFT calculations, ADME and td-Molecular dynamics simulations

Madhur Babu Singh [a,b], Pallavi Jain [b,**], Jaya Tomar [a], Vinod Kumar [c], Indra Bahadur [d], Dinesh Kumar Arya [e], Prashant Singh [a,*]

[a] Department of Chemistry, Atma Ram Sanatan Dharma College, University of Delhi, New Delhi, India
[b] Department of Chemistry, Faculty of Engineering and Technology, SRM Institute of Science and Technology, Delhi NCR Campus, Modinagar, Uttar Pradesh, India
[c] SCNS, Jawaharlal Nehru University, New Delhi, India
[d] Department of Chemistry, Faculty of Natural and Agricultural Sciences, North-West University, South Africa
[e] Department of Chemistry, Acharya Narendra Dev College, University of Delhi, New Delhi, India

ARTICLE INFO

Keywords:
Molecular dynamics simulations
Molecular docking
DFT studies
ADME
Repurposing drugs
Mpro of nCoV

ABSTRACT

In the present work, we have designed three molecules, acyclovir (A), ganciclovir (G) and derivative of hydroxymethyl derivative of ganciclovir (CH_2OH of G, that is D) and investigated their biological potential against the Mpro of nCoV via *in silico* studies. Further, density functional theory (DFT) calculations of A, G and D were performed using Gaussian 16 on applying B3LYP under default condition to collect the information for the delocalization of electron density in their optimized geometry. Authors have also calculated various energies including free energy of A, G and D in Hartree per particle. It can be seen that D has the least free energy. As mentioned, the molecular docking of the A, G and D against the Mpro of nCoV was performed using iGemdock, an acceptable computational tool and the interaction has been studied in the form of physical data, that is, binding energy for A, G and D were calculated in kcal/mol. It can be seen the D showed effective binding, that is, maximum inhibition that A and G. For a better understanding for the inhibition of the Mpro of nCoV by A, G and D, temperature dependent molecular dynamics simulations were performed. Different trajectories like RMSD, RMSF, Rg and hydrogen bond were extracted and analyzed. The results of molecular docking of A, G and D corroborate with the td-MD simulations and hypothesized that D could be a promising candidate to inhibit the activity of Mpro of nCoV.

1. Introduction

Drug repurposing is the concept of utilising the FDA-approved drugs for a new problem, infection or illness other than the one for which it was originally approved. These repurposing drugs save the time and money, accelerated their admittance into experimental clinical trials against other diseases. This process involved the activity based on an experimental or computational approach to develop the new employ of a drug for its biological potency [1–3]. COVID-19 is named for coronavirus disease-19 and it can cause a range of illness from common cold to severe respiratory syndrome and also infects other organs of the body. Coronaviruses (CoV) are a family of encapsulated viruses with single-strained RNA and pathogen. In comparison of previously identified SARS-CoV (2002) and MERS-CoV (2013), SARS-CoV-2 or nCoV is a more virulent variant [4–7]. New SARS-CoV has recently received huge attention worldwide and has been declared as a public health emergency of global concern. Repurposing drug like acyclovir is a well-known antiviral drug and was approved for the treatment of infections due to herpes viruses and zoster virus. A clinical research report has been published, showing the acyclovir as a promising drug against the infection due to SARS-CoV-2 [8]. Heidary et al. has reported a study for acyclovir to be a potential candidate against COVID-19 [9]. Acyclo-GTP is a more efficient inhibitor of viral DNA. Ganciclovir and acyclovir have shown good efficacy against cytomegalovirus infection [10]. A case has

* Corresponding author.
** Corresponding author.
E-mail addresses: palli24@gmail.com (P. Jain), psingh@arsd.du.ac.in (P. Singh).

https://doi.org/10.1016/j.jics.2022.100433
Received 19 January 2022; Received in revised form 8 March 2022; Accepted 17 March 2022
Available online 18 March 2022
0019-4522/© 2022 Indian Chemical Society. Published by Elsevier B.V. All rights reserved.

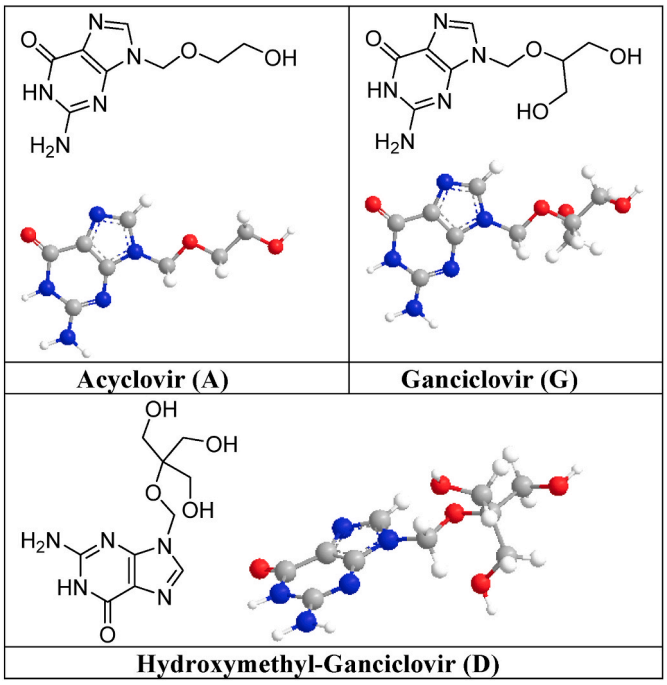

Fig. 1. Structures of A, G and D

reported that ganciclovir may act as an effective antiviral drug even against SARS-CoV-2 [11].

Molecular docking provide the preliminary information for the interaction of small molecules with the receptors. Various tools are available to perform molecular docking. Molecular dynamics (MD) simulations in drug development played an important role. The behaviour of proteins and other biomolecules is captured in atomic resolution in the presence or absence of small molecules. Khan et al. has performed MD simulation of drugs to cure HIV as a potent inhibitor for Mpro of nCoV [12]. DFT calculations helps in predicting stability of the compound via calcuating energies of the optimized geometry. With the help of DFT calculations, the dipole moment and enthalpy of formation can be calculated and these would help us to conclude about the molecule's polarity and behaviour. If the dipole moment of molecule is high then it is considered to be polar, means it could be more water-soluble and may be considered as probable candidate for oral delivery [13,14]. Preliminary information for the binding affinity between the Mpro of nCoV and ligands can be determined using iGemdock 2.1, an acceptable computational tool [15]. There is a possibility of various interaction mainly van der Waals interaction, hydrogen bonding. Our research group has performed preliminary information about the molecular docking of acyclovir and its derivatives with Mpro of nCoV; are based on the standard docking as a preprint [16]. The molecular docking of acyclovir and its derivative against the Mpro of nCoV and their binding energy are −89.64 and −96.21 kcal/mol respectively [17]. Absorption, Distribution, Metabolism and Excretion (ADME) is important for every chemist to know the suitability of a molecule as a promisng candidate. ADME is used to filter the compounds to get the leading molecule. In this work, acyclovir (A), ganciclovir, (G) and hydroxymethyl derivative of ganciclovir (D) are taken for study to inhibit the activity of main protease (Mpro) of novel corona virus (CoV) using molecular docking and DFT calculations is performed to know the electronic behaviour of molecules. Further to make the information obtained based on molecular docking reliable, molecular dynamics (MD) simulations of Mpro of nCoV with designed molecules at different temperature.

Table 1
Binding energy of different docked poses of acyclovir (A), ganciclovir (G) and hydroxymethyl-ganciclovir (D).

S. No	Ligand	Total Energy	Ligand	Total Energy	Ligand	Total Energy
1	A-0	−104.785	G-0	−109.324	D-0	−118.124
2	A −1	−103.521	G-1	−110.567	D-1	−118
3	A −2	−104.53	G-2	−107.279	D-2	−112.417
4	A-3	−103.388	G-3	−110.605	D-3	−113.368
5	A-4	−103.05	G-4	−109.548	**D-4**	**−119.226**
6	A-5	−103.917	G-5	−109.292	D-5	−113.106
7	A-6	−105.054	G-6	−109.132	D-6	−114.796
8	A-7	−105.068	G-7	−108.602	D-7	−116.265
9	A-8	−104.73	G-8	−107.609	D-8	−114.076
10	A-9	−103.084	G-9	−107.915	D-9	−109.424

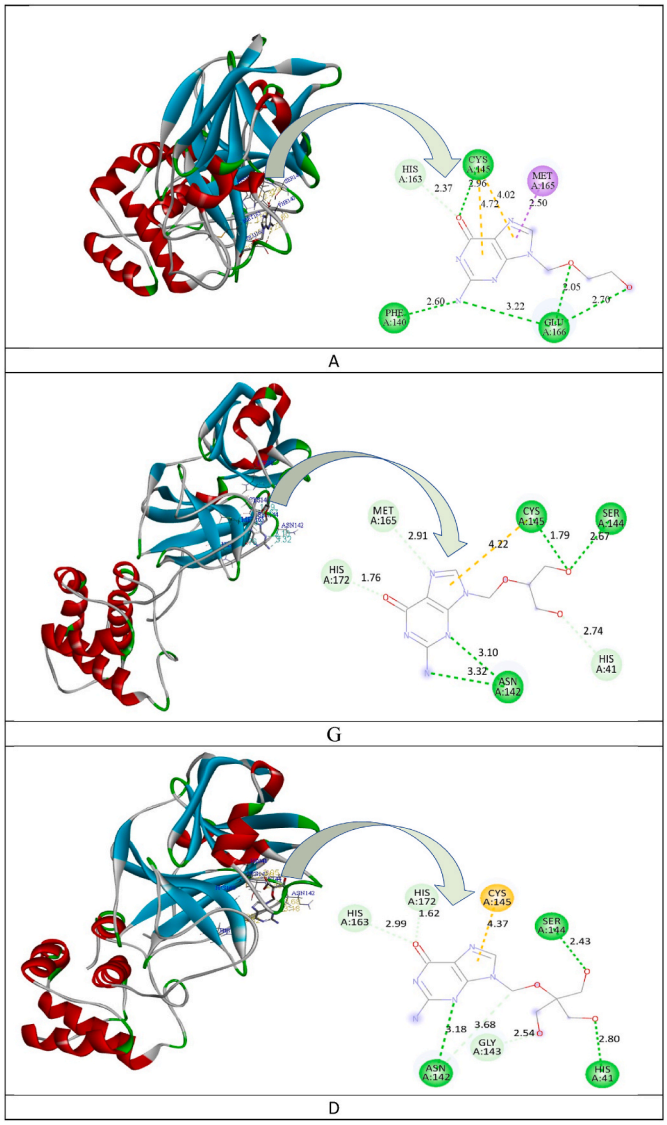

Fig. 2. Three dimensional and two-dimensional docked view of A, G and D with Mpro of nCoV.

2. Theoretical calculations

2.1. Designing of ligands

Structures of acyclovir, ganciclovir and hydroxymethyl-ganciclovir are drawn using chemdraw as in Fig. 1.

Table 2
Different types of interaction of A, G and D with the amino-acids of Mpro of nCoV.

Ligand	H-Bond				Hydrophobic	
	Classical		Non-classical			
	Amino Acid	Distance (Å)	Amino Acid	Distance (Å)	Amino Acid	Distance (Å)
A	PHE-140	2.60	HIS-163	2.37	MET-165	2.50
	GLU-166	2.05, 2.70, 3.22				
	CYS-145	2.96				
G	ASN-142	3.10, 3.32	HIS-172	1.76		
	SER-144	2.67	MET-165	2.91		
	CYS-145	1.79	HIS-41	2.74		
D	SER-144	2.43	GLY-143	2.54		
	ASN-142	3.18	HIS-172	1.62		
	HIS-41	2.80	ASN-142	3.68		
			HIS-163	2.99		
			HIS-41	3.05		

2.2. Molecular docking

The crystal structure for Mpro of nCoV is taken from the RCSB (PDB:6LU7). Before performing molecular docking and molecular dynamics simulations, the structure is prepared using chimera. For this, the structure of the said protease was opened in chimera followed by removal of ligand, water molecules and heteroatoms were deleted to make docking successful and the structure was then saved in PDB format for its further use [18–20]. The structures of all the three ligands were optimized by applying MM2 forcefield before performing molecular docking. The docking (very slow - 10 poses obtained for each ligand) was performed using iGemdock 2.1 and gives interaction in physical data, that is, binding energy in kcal/mol as in Table 1. BIOVIA Discovery Studio Visualizer was used to examine the results ontained and the docked views are given in Fig. 2 [21].

2.3. DFT calculation

DFT calculations of A, G and D were performed by using Gaussian 16.0 and Gaussview 6, act as an interface of gaussian to run the calculations on window [22,23]. The parameter applied to perform calculation are optimization plus frequency with B3LYP; the basis set selected was 6-311G (d,p) at 298 K [24,25].

2.4. Molecular dynamics (MD) simulations

MD simulations of Mpro of nCoV with A, G and D are performed at various temperatures (290, 300, 310 and 320 K) with the help of an online web server, WebGro (https://simlab.uams.edu/) and it uses GROMACS to perform the calculations [26–30]. This online server is available for the academic people. Input parameters for performing the calculations are: forcefield of GROMACS9643a, box type is triclinic, water model is SPC and salt type is NaCl. Equilibration and MD simulations run parameter used are pressure (1bar), number of frames per simulation 1000 and simulation time (100 ns) [31,32]. The GlycoBioChem PRODRG2 is an online server (http://davapc1.bioch.dundee.ac.uk/cgi-bin/prodrg) was used to create topology of small molecules for performing MD simulations [33].

2.5. Absorption, distribution, Metabolism and Excretion (ADME) of A, G and D

It is reported that a molecule may be a considered as a drug if it has the ability to reach its target with sufficient amount and should be active in the body for the appropriate time. In the present work, a free and acceptable online server, that is, swissADME (http://www.swissadme.ch) has been used to calculate various physiochemical and pharmacokinetic properties of the designed A, G and D.

3. Result and discussion

3.1. Molecular docking of A, D ang G

The docked poses of A, G and D with Mpro of nCoV in the two and three-dimensional view to know different types of the molecular interaction are given in Fig. 2. 3D views generally focused on the fitting of the

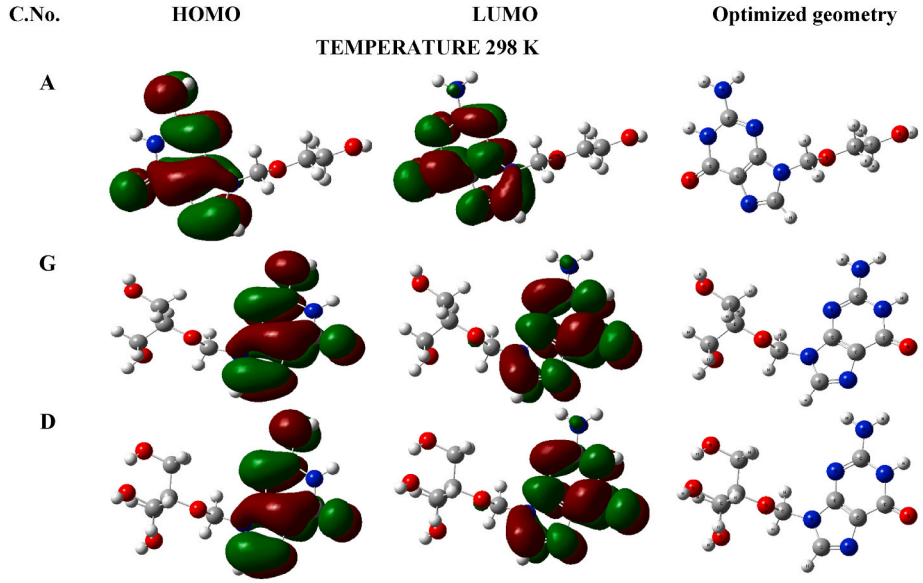

Fig. 3. HOMO, LUMO and Optimized geometry structures of A, G and D.

Table 3
Thermodynamic parameters of A, G and D.

Compound	Sum of electronic and zero-point Energies (Hartree per particle)	Sum of electronic and thermal Energies (Hartree per particle)	Sum of electronic and thermal Enthalpies (Hartree per particle)	Sum of electronic and thermal Free Energies (Hartree per particle)	Optimization energy (Hartree per particle)	Dipole moment (a. u.)
A	−810.66964	−810.65477	−810.65382	−810.65382	−810.880213	9.7791
G	−925.16575	−925.14840	−925.14746	−925.21332	−925.40877	10.4241
D	−1039.66047	−1039.6412	−1039.64026	−1039.7090	−1039.93684	8.9611

Table 4
Physio-chemical descriptors of A, G and D.

Compound	E_{LUMO}	E_{HOMO}	$E_{HOMO-LUMO}$	$E_{LUMO+HOMO}$	η	χ	S	μ	Ω
A	−0.0297	−0.2252	−0.1955	−0.2549	−0.0978	0.12745	−5.1154	−0.1275	−0.0831
D	−0.0297	−0.2251	−0.1953	−0.2548	−0.0977	0.12740	−5.1201	−0.127	−0.0831
G	−0.0294	−0.2245	−0.1951	−0.2538	−0.0975	0.12692	−5.1264	−0.1269	−0.0826

molecular in the cavity and conventional Hydrogen bonding while the 2D views explain various interactions like non-conventional hydrogen bonding, hydrophobic interaction, electrostatic, etc. Interaction of the A, D and G with different amino acids of Mpro of nCoV with the distance are given in Table 2. Docking analysis shows that A forms classical hydrogen bonding with PHE-140 (2.60), GLU-166 (3.22, 2.05, 2.70) and with CYS-145 (2.96); D forms conventional hydrogen bonds with SER-144 (2.43), CYS-145 (4.37), G forms hydrogen bonds with SER-144 (2.67), CYS-145 (4.22, 1.79) and ASN (3.22, 3.10).

3.2. DFT calculations

Using the DFT calculations, different thermodynamic parameters like enthalpy, free energy, optimization energy, thermal energy and zero-point energy have been calculated. HOMO determined can be used to find electron rich site [34] and LUMO is the one indicate the electron defficient site [35]. It is important to mention that higher the energy of HOMO means has more ability to donate electron density. HUMO, LUMO and optimized geometry of A, G and D are given in Fig. 3.

Further, different thermodynamics parameter such as zero-point energy, thermal energy, Optimization energy and thermal enthalpy are calculated in Jartree per particle and no significant changes is found these enegies as in Table 3. Free energies of the molecules is an important parameter to know the stability of a compound. It is considered that lesser the free energy of molecule indicates higher stability [34,36–38]. Among all the designed compounds, D has the lowest free energy, that is, −1039.7090 (Hartree per particle) and is considered to be more stable. Dipole moment is also an important parameter for predicting the solubility in polar solvents. Table 3 shows that G has the maximum dipole moment of 10.4241 a.u. in compounds taken.

Various physiochemical descriptors were also determined for the above reported three molecules by DFT calculation as given in Table 4. E_{LUMO} and E_{HOMO} are significant chemical factors for determining a molecules reactivity and are also applied to derive a range of important chemical reactivity descriptors such as chemical hardness (η), chemical potential (μ), softness(S), electronegativity (χ) are reported in Table 4. Energy gap of HOMO and LUMO is a useful parameter for determining the reactivity of compound. The charge-transfer interaction between the acceptor and donor groups is readily seen in the energy gap of the molecule. The E_{HOMO}–E_{LUMO} energy gap can be used to determine whether a molecule is soft or hard. The existence of a significant energy-gap identifies the molecule as a hard molecule, whereas less energy gap defines the molecule as a soft molecule. Table 4 shows that A has minimum energy gap of −0.1955 and G has maximum of −0.1951. Soft molecules have more polarizability than hard one because they need less energy for excitation. Chemical hardness of A, D and G are found to be −0.0978, −0.0977, −0.0975 respectively. As chemical hardness decreases the stability of compound decreases and polarizability increase.

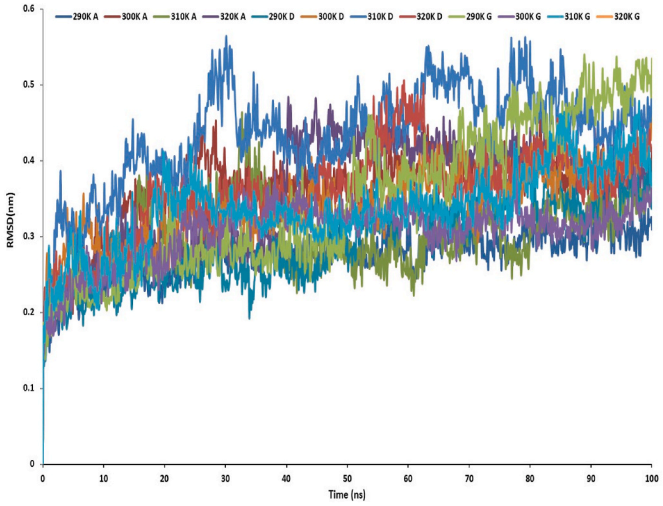

Fig. 4. Trajectory of RMSD fit to backbone for the Mpro of nCoV with A, G and D at 290, 300, 310 and 320 K.

Based on these data, D is considered to be less polarizable than G. Electronegativity defines the tendency of compound to attract the shared pair of electrons and it is the difference of electron affinity and ionization potential. Obtained data shows that A has highest electronegativity value of −0.12745 and G has minimum of −0.12692. Chemical potential refers to a substance's capacity to generate a chemical reaction in its environment as a result of its own chemical energy or external energy as given in Table 4. Mathematically, chemical potential is negative or reverse of the electronegativity of the compound. The energies of HOMO and LUMO are directly related to the ionization potential and electron affinity respectively.

3.3. Molecular dynamics simulations

MD simulations is used to analyze the dynamic of macromolecular system in presence of small molecule. Various trajectories are obtained from the results of MD simulations and gives useful information to explore the protein-ligand interactions [39,40]. MD simulations of Mpro of nCoV with A, G and D were performed for 100 ns at different temperature. Root mean square deviation (RMSD) trajectory is the measure of the average square root of deviation from the mean distance of the complex, that is, protein-ligand complex [41,42]. It provides the conformational stability of macromolecular system due to the binding of ligand into the active cavity of rector. RMSD values ranges between 0.35 nm is considered to be acceptable. It was also found that on

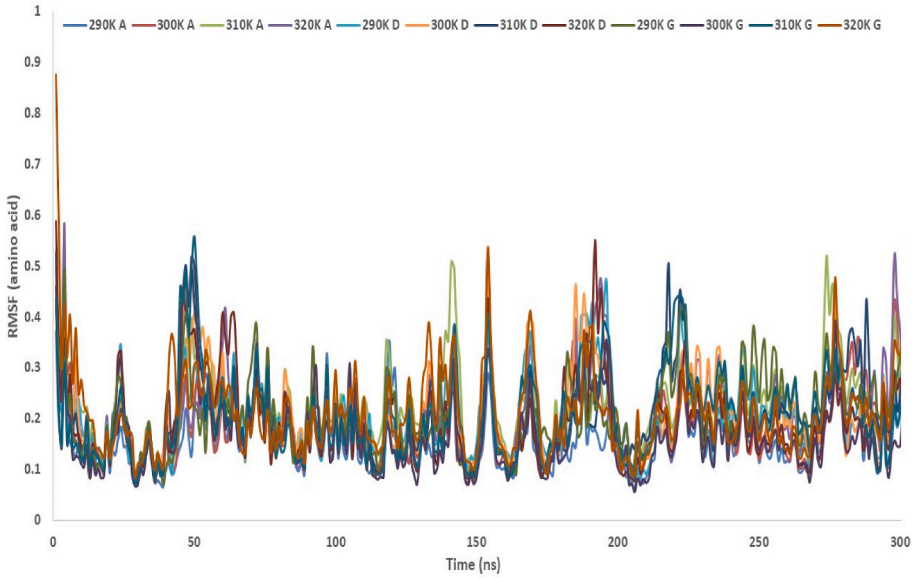

Fig. 5. Trajectory of RMSF for the Mpro of nCoV with A, G and D at 290, 300, 310 and 320 K.

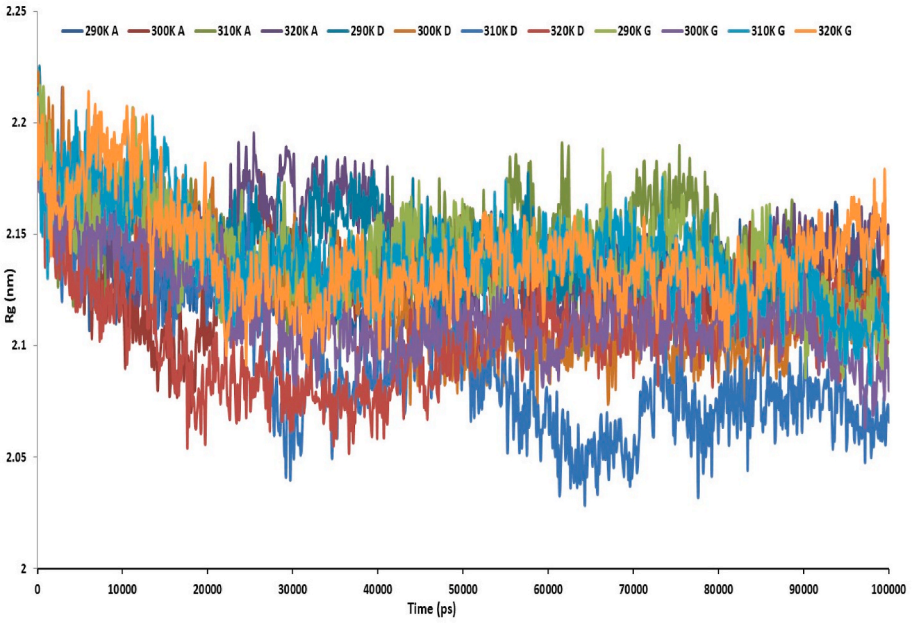

Fig. 6. Trajectory of radius of gyration for the Mpro of nCoV with A, G and D at 290, 300, 310 and 320 K.

increasing temperature the RMSD value increases. Lower temperature favors stabilization of protein-ligand complex (Fig. 4).

Root mean square fluctuation (RMSD) is used to study the fluctuation values of the atomic coordinates of the atoms of amino acids in presence of ligand (A, D and G) [43]. Fluctuations values were used to analyze the configurational changes of the protease at different temperature. RMSF graphs for the protein with A, G and D were analyzed as in Fig. 5. From the analysis, fluctuations were recorded in a range of 140–160, 40–60, 160–180, 240–260 amino acids.

Radius of gyration is the measure of the distance between center of mass and axis of rotation of the protease -ligand complex. Lesser the value of radius of gyration indicates higher the stability of the complex [44,45]. Radius of gyration values was analyzed for the Mpro of nCoV in presence of A, G and D at different temperature (Fig. 6). At low temperature, radius of gyration is less and indicates higher stability. But an increasing temperature for MD simulations, the value of Rg of the complex increases and thus, the stability decreases. Results of molecular docking corroborate with the results obtained by MD simulations.

Number of hydrogen bonds play a significant role to understand the stability of the formed complex. The anchoring becomes tighter as the number of hydrogen bonds increases and the length of hydrogen bond decreases [46,47]. The number of hydrogen bonds and their persistency were analyzed during simulation at different temperatures as given in Fig. 7. Maximum number of hydrogen bonds found are six in case of A while for D and G, the maximum hydrogen bonds are five. The number of hydrogen bonds alone cannot decide the stability of the complex.

3.4. Absorption, distribution, Metabolism and Excretion (ADME) of A, G and D

ADME characteristics are important in the drug development process [48]. Generally, about 50% of the drugs like candidates fails due to

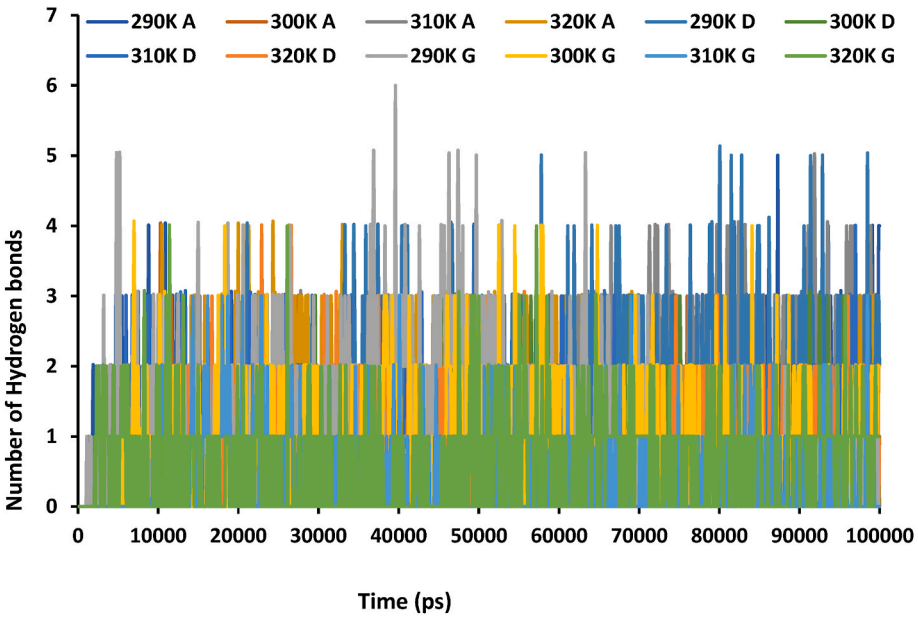

Fig. 7. Trajectory of H-bond for the Mpro of nCoV with A, G and D at 290, 300, 310 and 320 K.

Table 5
Physiochemical properties of acyclovir (A), ganciclovir (G) and hydroxymethyl-ganciclovir (D).

Physiochemical properties	Acyclovir (A)	Ganciclovir (G)	Derivative of acyclovir (D)
Log S	−0.41	−0.42	0.37
Solubility	Very soluble	Very soluble	Highly soluble
Heavy atoms	16	18	20
Molecular weight (g/mol)	225.20	255.23	285.26
No. of rotational bonds	4	5	6
No. H-bond acceptors	5	6	7
Num. H-bond donors	3	4	5
Log $P_{o/w}$ (WLOGP)	−1.48	−2.11	−2.75
Physiochemical space for oral bioavailability			

insufficient effectiveness like low bioavailability due to inadequate intestinal absorption and poor metabolic stability [49–52]. Lipophilicity is the partition coefficient of a molecule between the n-octanol and water (log $P_{O/W}$) and used to understand the solubility of the molecules or compounds in the water v/s organic solvent [53]. The partition coefficient is a significant indicator of a substance physical constitution and determines its behavior in various situation. For an effective drug, the value of log $P_{O/W}$ is less than or equal to 5 [54]. Solubility is an important criterion in deciding a molecule to be drug, therefore, log S should be less than 6. According to Lipinski's rule of five, an orally active drug must have: (i) hydrogen bond donor less than or equal to five (ii) hydrogen bond acceptor less than or equal to ten (iii) molecular mass less than 500 g/mol (iv) log P values less than 5 [55–58]. Table 5 shows the physiochemical properties of A, G and D. All the studied molecules obey the Lipinski rule of 5.

Drug likeness is an important criterion for evaluating the behavior of molecule during early stage of drug development. This factor may be regarded as a way to link physicochemical properties of a compound with the biopharmaceutical properties in the human body for oral delivery. Despite the fact that there are several methods for delivery of drugs, oral delivery approach is favored for patient. At various stages of the discovery process, early assessment of oral bioavailability i.e. the percentage of the dosage that reaches the blood following oral administration is a significant decision-making factor. Bioavailability of a molecule is influenced by many factors and the gastrointestinal (GI) absorption considered to play most significant role important. The BBB (blood-brain barrier) may be regarded as a shield that protects the brain through a "physical" barrier and a "biochemical" barrier (e.g. P glycoprotein pumping out substrate from CNS tissues). **BBB** ensures the consistency of central nervous system (CNS) on allowing brain tissues to interchange nutrients with the outside world [59]. We uderstand the importance of active transport but passive diffusion is the primary path for a drug like candidate to reach the brain via blood. The approach to evaluate the active efflux through biological membrane (GI wall) to the brain. P-gp has many functions like protection of CNS from xenobiotics. TPSA is a key characteristic for drug likeness and its value must be smaller than 130 Å. In Table 6, bioactivity and drug likeness score of A, G and D are mentioned. A shows high GI absorption due to the TPSA value of 119.06 Å [60,61]. G and D have TPSA have TPSA value of more than 130 Å and less GI absorption [62].

4. Conclusion

Herein, the authors have designed three candidate and out of them, acyclovir (A) and ganciclovir (G) are well know and a hydroxymethyl derivative of ganciclovir (D) is created. Then, they were docked against the Mpro of nCoV using iGemdock. The binding energy of A, G and D are −105.068, −110.65 and −119.226 kcal/mol, respectively. D has a

Table 6
Bioactivity and drug likeness score of acyclovir, ganciclovir and hydroxymethyl-ganciclovir.

C. No.	GI absorption	BBB permeant	Lipinski rule	Log K_p (skin permeation) (cm/s)	TPSA (Å)	P-gp substrate
A	High	No	Yes; 0 violation	−8.78	119.06	No
G	Low	No	Yes; 0 violation	−9.04	139.29	No
D	Low	No	Yes; 0 violation	−10.20	159.52	No

minimum binding energy of −119.226 kcal/mol, means it could be a promising inhibitor against Mpro of nCoV. For a better understanding for the inhibition, authors have performed temperature dependent MD simulation of Mpro of nCoV with A, G and D using WebGro at 290, 300, 310 and 320 K. MD simulations corroborates with docking results. Further, DFT calculations of A, G and D are performed using Gaussian 16 to see the localization of electron density and stability. Result shows that D has minimum free energy of −1039.7090 Hartree per particle. Further, ADME properties of A, G and D were calculated using swissADME to evaluate solubility, bioavailability and potential of the molecules to become an effective drugs. It has been found that A, G and D followed the Lipinski rule with no violation and falls in an acceptable range for their bioavailability.

Funding

There is no source of financial support to perform the work.

Disclosure of potential conflicts of interest and informed consent

I further confirm that the order of authors listed in the manuscript has been approved by all of us. The authors have relevant financial and non-financial interests to disclose. A draft of this was previously submitted to the ResearchSquare platform as a preprint (https://assets.researchsquare.com/files/rs-1250241/v1/cd2c5edf-2725-4029-83e0-624e60b30507.pdf?c=1642437790).

Availability of data and material

"The datasets generated during and/or analyzed during the current study are available from the corresponding author on reasonable request."

Code availability

N/A.

Authors' contributions

"All authors contributed to the study conception and design. Material preparation, data collection and analysis were performed by [Madhur Babu Singh], [Dinesh Kumar Arya], [Jaya Tomar] and [Pallavi Jain]. The manuscript was written by [Indra Bahadur], [Prahsant Singh] and [Vinod Kumar]. All authors read and approved the final manuscript."

Research involving human participants and/or animals

It is declared that no human participants and/or animals are used in this work.

Declaration of competing interest

I, Dr. Prashant Singh, on behalf of the all the authors declare that there is no potential conflict of interest on the manuscript titled "An ***In Silico*** investigation **for Acyclovir and its derivatives to fight the COVID-19: Molecular docking, DFT calculations, ADME and td-Molecular dynamics simulations study for Acyclovir, Ganciclovir and its derivatives to fight the COVID-19: Molecular docking, DFT calculations, ADME and td-Molecular dynamics simulations**".

References

[1] M. Phadke, S. Saunik, COVID-19 treatment by repurposing drugs until the vaccine is in sight, Drug Dev. Res. 81 (2020) 541–543, https://doi.org/10.1002/ddr.21666.

[2] P. Schlagenhauf, M.P. Grobusch, J.D. Maier, P. Gautret, Repurposing antimalarials and other drugs for COVID-19, Travel Med, Inf. Disp. 34 (2020) 101658, https://doi.org/10.1016/j.tmaid.2020.101658.

[3] S.N. Deftereos, C. Andronis, E.J. Friedla, A. Persidis, A. Persidis, Drug repurposing and adverse event prediction using high-throughput literature analysis, WIREs Syst. Biol. Med. 3 (2011) 323–334, https://doi.org/10.1002/wsbm.147.

[4] R. Mann, A. Perisetti, M. Gajendran, Z. Gandhi, C. Umapathy, H. Goyal, Clinical characteristics, diagnosis, and treatment of major coronavirus outbreaks, Front. Med. 7 (2020) 766, https://doi.org/10.3389/fmed.2020.581521.

[5] A. Nassar, I.M. Ibrahim, F.G. Amin, M. Magdy, A.M. Elgharib, E.B. Azzam, F. Nasser, K. Yousry, I.M. Shamkh, S.M. Mahdy, A.A. Elfiky, A review of human coronaviruses' receptors: the host-cell targets for the crown bearing viruses, Molecules 26 (2021), https://doi.org/10.3390/molecules26216455.

[6] A. Rahimi, A. Mirzazadeh, S. Tavakolpour, Genetics and genomics of SARS-CoV-2: a review of the literature with the special focus on genetic diversity and SARS-CoV-2 genome detection, Genomics 113 (2021) 1221–1232, https://doi.org/10.1016/j.ygeno.2020.09.059.

[7] A.A.T. Naqvi, K. Fatima, T. Mohammad, U. Fatima, I.K. Singh, A. Singh, S.M. Atif, G. Hariprasad, G.M. Hasan, M.I. Hassan, Insights into SARS-CoV-2 genome, structure, evolution, pathogenesis and therapies: structural genomics approach, Biochim. Biophys. Acta. Mol. Basis Dis. 1866 (2020) 165878, https://doi.org/10.1016/j.bbadis.2020.165878.

[8] V.S. Baker, Acyclovir for SARS-CoV-2 : an ClinicalPractice old drug with a new purpose, Clin. Pract. 18 (2021) 1584–1592.

[9] F. Heidary, S. Madani, R. Gharebaghi, F. Asadi-amoli, Acyclovir as a potential add-on therapy in COVID-19 treatment regimens, Pharmaceut. Sci. 27 (2021) S68–S77, https://doi.org/10.34172/PS.2021.38.

[10] D.R. Weller, H.H. Balfour Jr., H.E. Vezina, Simultaneous determination of acyclovir, ganciclovir, and (R)-9-[4-hydroxy-2-(hydroxymethyl)butyl]guanine in human plasma using high-performance liquid chromatography, Biomed. Chromatogr. 23 (2009) 822–827, https://doi.org/10.1002/bmc.1192.

[11] M. Ben Salem, L. Salima, H. Mouna, S.K. Taieb, I. Handous, B.S. Manel, L.S. Ahmed, A.S. Sabra, H. Skhiri, Immunosuppressive drugs and ganciclovir: two modalities to prevent COVID-19 severity: a case report, PAMJ Clin. Med. 5 (2021), https://doi.org/10.11604/pamj-cm.2021.5.86.28901.

[12] A. Khan, S.S. Ali, M.T. Khan, S. Saleem, A. Ali, M. Suleman, Z. Babar, A. Shafiq, M. Khan, D.-Q. Wei, Combined drug repurposing and virtual screening strategies with molecular dynamics simulation identified potent inhibitors for SARS-CoV-2 main protease (3CLpro), J. Biomol. Struct. Dyn. 39 (2021) 4659–4670, https://doi.org/10.1080/07391102.2020.1779128.

[13] Y.S. Mary, Y.S. Mary, S. Armaković, S.J. Armaković, R. Yadav, I. Celik, P. Mane, B. Chakraborty, Stability and reactivity study of bio-molecules brucine and colchicine towards electrophile and nucleophile attacks: insight from DFT and MD simulations, J. Mol. Liq. 335 (2021) 116192, https://doi.org/10.1016/j.molliq.2021.116192.

[14] S. Beegum, Y.S. Mary, Y.S. Mary, R. Thomas, S. Armaković, S.J. Armaković, J. Zitko, M. Dolezal, C. Van Alsenoy, Exploring the detailed spectroscopic characteristics, chemical and biological activity of two cyanopyrazine-2-carboxamide derivatives using experimental and theoretical tools, Spectrochim. Acta Part A Mol. Biomol. Spectrosc. 224 (2020) 117414, https://doi.org/10.1016/j.saa.2019.117414.

[15] M.P. Kumar, K.M. Sundaram, M.S. Ramasamy, Coronavirus spike (S) glycoprotein (2019-ncov) targeted siddha medicin es kabasura kudineer and thonthasura kudineer–in silico evidence for c orona viral drug, Asian J. Pharmaceut. Res. Health Care 12 (n.d.) 20–27.

[16] D. Kumar, A.R. Sanatan, K. Kumari, I. Bahadur, P. Singh, Promising Acyclovir and its Derivatives to Inhibit the Protease of SARS-CoV-2: Molecular Docking and Molecular Dynamics Simulations, Researchsquare, 2020, pp. 1–17. https://assets.researchsquare.com/files/rs-94864/v1/58b51f1c-16d2-4c9b-b498-e5e8950116fc.pdf?c=1631858552.

[17] B. Arunkumar, A. Fernandez, S.P. Laila, A.S. Nair, Molecular docking study of acyclovir and its derivatives as potent inhibitors in novel covid-19, Int. J. Pharma Sci. Res. 11 (2020) 4700, https://doi.org/10.13040/IJPSR.0975-8232.11(9).4700-05.

[18] B.J. Bender, S. Gahbauer, A. Luttens, J. Lyu, C.M. Webb, R.M. Stein, E.A. Fink, T. E. Balius, J. Carlsson, J.J. Irwin, B.K. Shoichet, A practical guide to large-scale docking, Nat. Protoc. 16 (2021) 4799–4832, https://doi.org/10.1038/s41596-021-00597-z.

[19] F.A. Ugbe, G.A. Shallangwa, A. Uzairu, I. Abdulkadir, Activity modeling, molecular docking and pharmacokinetic studies of some boron-pleuromutilins as anti-wolbachia agents with potential for treatment of filarial diseases, Chem. Data Collect. 36 (2021) 100783, https://doi.org/10.1016/j.cdc.2021.100783.

[20] S.K. Burley, H.M. Berman, G.J. Kleywegt, J.L. Markley, H. Nakamura, S. Velankar, Protein data bank (PDB): the single global macromolecular structure archive, in: A. Wlodawer, Z. Dauter, M. Jaskolski (Eds.), Protein Crystallogr. Methods Protoc., Springer New York, New York, NY, 2017, pp. 627–641, https://doi.org/10.1007/978-1-4939-7000-1_26.

[21] K.-C. Hsu, Y.-F. Chen, S.-R. Lin, J.-M. Yang, iGEMDOCK: a graphical environment of enhancing GEMDOCK using pharmacological interactions and post-screening analysis, BMC Bioinf. 12 (2011) S33, https://doi.org/10.1186/1471-2105-12-S1-S33.

[22] M.J. Frisch, G.W. Trucks, H.B. Schlegel, G.E. Scuseria, M.A. Robb, J.R. Cheeseman, G. Scalmani, V. Barone, G.A. Petersson, H. Nakatsuji, X. Li, M. Caricato, A. V. Marenich, J. Bloino, B.G. Janesko, R. Gomperts, B. Mennucci, H.P. Hratchian, J. V. Ortiz, A.F. Izmaylov, J.L. Sonnenberg, D. Williams-Young, F. Ding, F. Lipparini, F. Egidi, J. Goings, B. Peng, A. Petrone, T. Henderson, D. Ranasinghe, V.

G. Zakrzewski, J. Gao, N. Rega, G. Zheng, W. Liang, M. Hada, M. Ehara, K. Toyota, R. Fukuda, J. Hasegawa, M. Ishida, T. Nakajima, Y. Honda, O. Kitao, H. Nakai, T. Vreven, K. Throssell, J.A. Montgomery Jr., J.E. Peralta, F. Ogliaro, M. J. Bearpark, J.J. Heyd, E.N. Brothers, K.N. Kudin, V.N. Staroverov, T.A. Keith, R. Kobayashi, J. Normand, K. Raghavachari, A.P. Rendell, J.C. Burant, S.S. Iyengar, J. Tomasi, M. Cossi, J.M. Millam, M. Klene, C. Adamo, R. Cammi, J.W. Ochterski, R.L. Martin, K. Morokuma, O. Farkas, J.B. Foresman, D.J. Fox, Gaussian 16, Rev. C.01, Gaussian 16, Rev. C. 01, 2016.

[23] R. Dennington, T.A. Keith, J.M. Millam, GaussView Version 6, (n.d).

[24] J. Foresman, E. Frish, Exploring Chemistry, Gaussian Inc., Pittsburg, USA, 1996.

[25] E. Klein, V. Lukeš, M. Ilčin, DFT/B3LYP study of tocopherols and chromans antioxidant action energetics, Chem. Phys. 336 (2007) 51–57, https://doi.org/10.1016/j.chemphys.2007.05.007.

[26] H. Bekker, H.J.C. Berendsen, E.J. Dijkstra, S. Achterop, R. Vondrumen, D. Vanderspoel, A. Sijbers, H. Keegstra, M.K.R. Renardus, GROMACS - A PARALLEL COMPUTER FOR MOLECULAR-DYNAMICS SIMULATIONS, in: R.A. DeGroot, J. Nadrchal (Eds.), World Scientific Publishing, n.d.: pp. 252–256.

[27] M.J. Abraham, T. Murtola, R. Schulz, S. Páll, J.C. Smith, B. Hess, E. Lindah, Gromacs: high performance molecular simulations through multi-level parallelism from laptops to supercomputers, SoftwareX 1–2 (2015), https://doi.org/10.1016/j.softx.2015.06.001.

[28] K. Lindorff-Larsen, S. Piana, K. Palmo, P. Maragakis, J.L. Klepeis, R.O. Dror, D. E. Shaw, Improved side-chain torsion potentials for the Amber ff99SB protein force field, Proteins Struct. Funct. Bioinforma. 78 (2010), https://doi.org/10.1002/prot.22711.

[29] E. Lindahl, P. Bjelkmar, P. Larsson, M.A. Cuendet, B. Hess, Implementation of the charmm force field in GROMACS: analysis of protein stability effects from correction maps, virtual interaction sites, and water models, J. Chem. Theor. Comput. 6 (2010), https://doi.org/10.1021/ct900549r.

[30] C. Oostenbrink, A. Villa, A.E. Mark, W.F. Van Gunsteren, A biomolecular force field based on the free enthalpy of hydration and solvation: the GROMOS force-field parameter sets 53A5 and 53A6, J. Comput. Chem. 25 (2004), https://doi.org/10.1002/jcc.20090.

[31] V.K. Vishvakarma, M.B. Singh, P. Jain, K. Kumari, P. Singh, Hunting the Main Protease of SARS-CoV-2 by Plitidepsin: Molecular Docking and Temperature-dependent Molecular Dynamics Simulations, Amino Acids, 2021, https://doi.org/10.1007/s00726-021-03098-1.

[32] V.K. Vishvakarma, S. Pal, P. Singh, I. Bahadur, Interactions between main protease of SARS-CoV-2 and testosterone or progesterone using computational approach, J. Mol. Struct. (2021) 131965, https://doi.org/10.1016/J.MOLSTRUC.2021.131965.

[33] A.W. Schüttelkopf, D.M.F. van Aalten, {\\it PRODRG}: a tool for high-throughput crystallography of protein{–}ligand complexes, Acta Crystallogr. Sect. D. 60 (2004) 1355–1363, https://doi.org/10.1107/S0907444904011679.

[34] M.B. Singh, A. Kumar, P. Jain, P. Singh, K. Kumari, An insight of novel eutectic mixture between thiazolidine-2,4-dione and zinc chloride: temperature-dependent density functional theory approach, J. Phys. Org. Chem.. n/a (n.d.) e4305. https://doi.org/10.1002/poc.4305.

[35] S. Song, M.-C. Kim, E. Sim, A. Benali, O. Heinonen, K. Burke, Benchmarks and reliable DFT results for spin gaps of small ligand Fe(II) complexes, J. Chem. Theor. Comput. 14 (2018) 2304–2311, https://doi.org/10.1021/acs.jctc.7b01196.

[36] A. Kumar, K. Kumari, A.P.S. Raman, P. Jain, D. Kumar, P. Singh, An insight for the interaction of drugs (acyclovir/ganciclovir) with various ionic liquids: DFT calculations and molecular docking, J. Phys. Org. Chem. (2021), https://doi.org/10.1002/poc.4287.

[37] A. Kumar, K. Kumari, I. Bahadur, P. Singh, Temperature dependent DFT studies to understand the physiochemical interaction of lithium chloride cluster ions in presence of syringic acid, J. Chem. Thermodyn. 152 (2021), https://doi.org/10.1016/j.jct.2020.106277.

[38] A. Singh, S. Singh, S. Sewariya, N. Singh, P. Singh, A. Kumar, R. Bandichhor, R. Chandra, Stereospecific N-acylation of indoles and corresponding microwave mediated synthesis of pyrazinoindoles using hexafluoroisopropanol, Tetrahedron 84 (2021), https://doi.org/10.1016/j.tet.2021.132017.

[39] Z. Chen, J. Yi, H. Zhao, H. Luan, M. Xu, L. Zhang, D. Feng, Strength development and deterioration mechanisms of foamed asphalt cold recycled mixture based on MD simulation, Construct. Build. Mater. 269 (2021) 121324, https://doi.org/10.1016/j.conbuildmat.2020.121324.

[40] R. Shukla, T. Tripathi, in: D.B. Singh (Ed.), Molecular Dynamics Simulation of Protein and Protein–Ligand Complexes BT - Computer-Aided Drug Design, Springer Singapore, Singapore, 2020, pp. 133–161, https://doi.org/10.1007/978-981-15-6815-2_7.

[41] I. Aier, P.K. Varadwaj, U. Raj, Structural insights into conformational stability of both wild-type and mutant EZH2 receptor, Sci. Rep. 6 (2016) 34984, https://doi.org/10.1038/srep34984.

[42] W. Schreiner, R. Karch, B. Knapp, N. Ilieva, Relaxation estimation of RMSD in molecular dynamics immunosimulations, Comput. Math. Methods Med. 2012 (2012) 173521, https://doi.org/10.1155/2012/173521.

[43] K. Sargsyan, C. Grauffel, C. Lim, How molecular size impacts RMSD applications in molecular dynamics simulations, J. Chem. Theor. Comput. 13 (2017) 1518–1524, https://doi.org/10.1021/acs.jctc.7b00028.

[44] G.C. Justino, C.P. Nascimento, M.C. Justino, Molecular dynamics simulations and analysis for bioinformatics undergraduate students, Biochem. Mol. Biol. Educ. 49 (2021) 570–582, https://doi.org/10.1002/bmb.21512.

[45] J. Zhu, Y. Lv, X. Han, D. Xu, W. Han, Understanding the differences of the ligand binding/unbinding pathways between phosphorylated and non-phosphorylated ARH1 using molecular dynamics simulations, Sci. Rep. 7 (2017) 12439, https://doi.org/10.1038/s41598-017-12031-0.

[46] I. Chikalov, P. Yao, M. Moshkov, J.-C. Latombe, Learning probabilistic models of hydrogen bond stability from molecular dynamics simulation trajectories, BMC Bioinf. 12 (2011) S34, https://doi.org/10.1186/1471-2105-12-S1-S34.

[47] R.B. Sessions, N. Gibbs, C.E. Dempsey, Hydrogen bonding in helical polypeptides from molecular dynamics simulations and amide hydrogen exchange analysis: alamethicin and melittin in methanol, Biophys. J. 74 (1998) 138–152, https://doi.org/10.1016/S0006-3495(98)77775-6.

[48] E. Cannady, K. Katyayan, N. Patel, Chapter 3 - ADME principles in small molecule drug discovery and development: an industrial perspective, in: W.M. Haschek, C. G. Rousseaux, M.A. Wallig, B. Bolon (Eds.), Haschek Rousseaux's Handb. Toxicol. Pathol., fourth ed., fourth ed., Academic Press, 2022, pp. 51–76, https://doi.org/10.1016/B978-0-12-821044-4.00003-0.

[49] T. Prueksaritanont, C. Tang, ADME of biologics—what have we learned from small molecules? AAPS J 14 (2012) 410–419, https://doi.org/10.1208/s12248-012-9353-6.

[50] A. Daina, O. Michielin, V. Zoete, SwissADME: a free web tool to evaluate pharmacokinetics, drug-likeness and medicinal chemistry friendliness of small molecules, Sci. Rep. 7 (2017) 42717, https://doi.org/10.1038/srep42717.

[51] A. Daina, V. Zoete, A BOILED-egg to predict gastrointestinal absorption and brain penetration of small molecules, ChemMedChem 11 (2016) 1117–1121, https://doi.org/10.1002/cmdc.201600182.

[52] A. Daina, O. Michielin, V. Zoete, iLOGP: a simple, robust, and efficient description of n-octanol/water partition coefficient for drug design using the GB/SA approach, J. Chem. Inf. Model. 54 (2014) 3284–3301, https://doi.org/10.1021/ci500467k.

[53] H. Özkan, Ş. Adem, Synthesis, Spectroscopic characterizations of novel norcantharimides, their ADME properties and docking studies against COVID-19 mpr, ChemistrySelect 5 (2020) 5422–5428, https://doi.org/10.1002/slct.202001123.

[54] S. Deb, A.A. Reeves, R. Hopefl, R. Bejusca, ADME and pharmacokinetic properties of remdesivir: its drug interaction potential, Pharmaceuticals 14 (2021), https://doi.org/10.3390/ph14070655.

[55] A.K. Ghose, V.N. Viswanadhan, J.J. Wendoloski, A knowledge-based approach in designing combinatorial or medicinal chemistry libraries for drug discovery. 1. A qualitative and quantitative characterization of known drug databases, J. Comb. Chem. 1 (1999) 55–68, https://doi.org/10.1021/cc9800071.

[56] W.J. Egan, M. Merz Kenneth, J.J. Baldwin, Prediction of drug absorption using multivariate statistics, J. Med. Chem. 43 (2000) 3867–3877, https://doi.org/10.1021/jm000292e.

[57] C.A. Lipinski, F. Lombardo, B.W. Dominy, P.J. Feeney, Experimental and computational approaches to estimate solubility and permeability in drug discovery and development settings, Adv. Drug Deliv. Rev. 23 (1997) 3–25, https://doi.org/10.1016/S0169-409X(96)00423-1.

[58] C.A. Lipinski, Lead- and drug-like compounds: the rule-of-five revolution, Drug Discov. Today Technol. 1 (2004) 337–341, https://doi.org/10.1016/j.ddtec.2004.11.007.

[59] T. Terasaki, Quantitative expression of ADME proteins at the blood-brain barrier, Drug Metabol. Pharmacokinet. 32 (2017) S12, https://doi.org/10.1016/j.dmpk.2016.10.059.

[60] T. Sawamoto, S. Haruta, Y. Kurosaki, K. Higaki, T. Kimura, Prediction of the plasma concentration profiles of orally administered drugs in rats on the basis of gastrointestinal transit kinetics and absorbability, J. Pharm. Pharmacol. 49 (1997) 450–457, https://doi.org/10.1111/j.2042-7158.1997.tb06823.x.

[61] T. Kimura, K. Higaki, Gastrointestinal transit and drug absorption, Biol. Pharm. Bull. 25 (2002) 149–164, https://doi.org/10.1248/bpb.25.149.

[62] V.K. Vishvakarma, P. Singh, V. Kumar, K. Kumari, R. Patel, R. Chandra, Pyrrolothiazolones as potential inhibitors for the nsP2B-nsP3 protease of dengue virus and their mechanism of synthesis, ChemistrySelect 4 (2019), https://doi.org/10.1002/slct.201901119.